Science Advances
AAAS

Supplementary Materials for

Decoding the interplay between m^{6}A modification and stress granule stability by live-cell imaging

Qianqian Li *et al.*

Corresponding author: Qin Peng, pengqin@szbl.ac.cn

Sci. Adv. **10**, eadp5689 (2024)
DOI: 10.1126/sciadv.adp5689

This PDF file includes:

Figs. S1 to S7

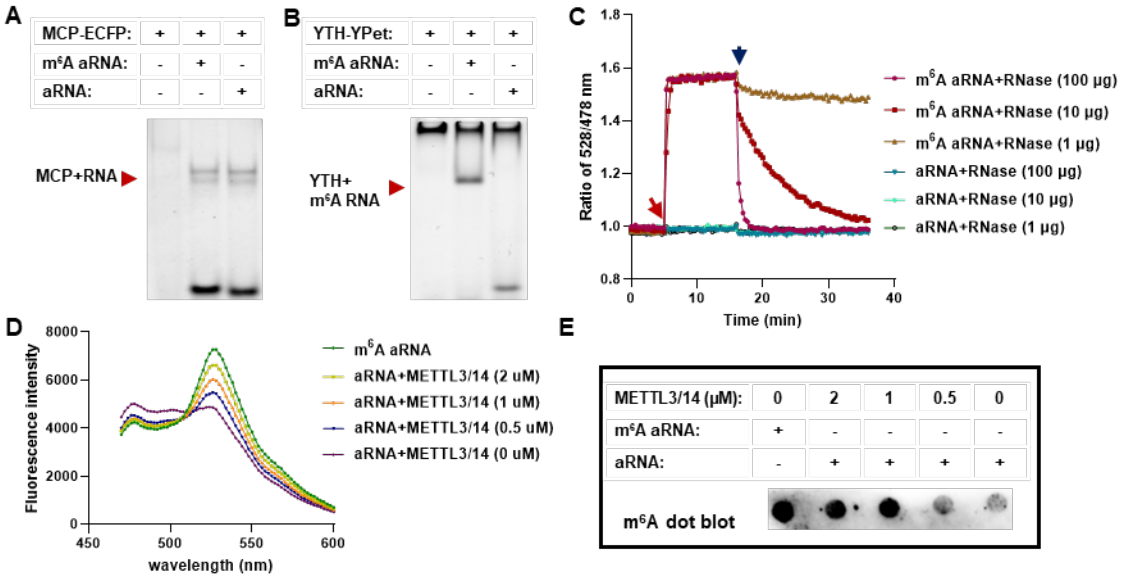

Fig. S1.

Verification of the specificity of the FRET system *in vitro*. (A) Gel red staining of native PAGE after MCP-ECFP was mixed with aRNA or m^{6}A aRNA, 1: MCP-ECFP; 2: MCP-ECFP + m^{6}A aRNA; 3: MCP-ECFP + aRNA; the arrow indicates the complex of MCP-ECFP with RNA. **(B)** Gel red staining of native PAGE after mixing YTH-YPet with aRNA or m^{6}A aRNA; 1: YTH-YPet; 2: YTH-YPet + m^{6}A aRNA; 3: YTH-YPet + aRNA; the arrow indicates the complex of YTH-YPet with m^{6}A RNA. **(C)** Ratio of 528/478 nm fluorescence after mixing MCP-ECFP and YTH-YPet; the red arrow indicates the addition of aRNA or m^{6}A aRNA, and the blue arrow indicates the addition of RNase at different concentrations. **(D)** Fluorescence spectrum after MCP-ECFP and YTH-YPet were mixed, aRNA or m^{6}A aRNA were added for 20 min, and METTL3/14 was added at different concentrations for 12 hr. **(E)** m^{6}A dot blot for **(D).**

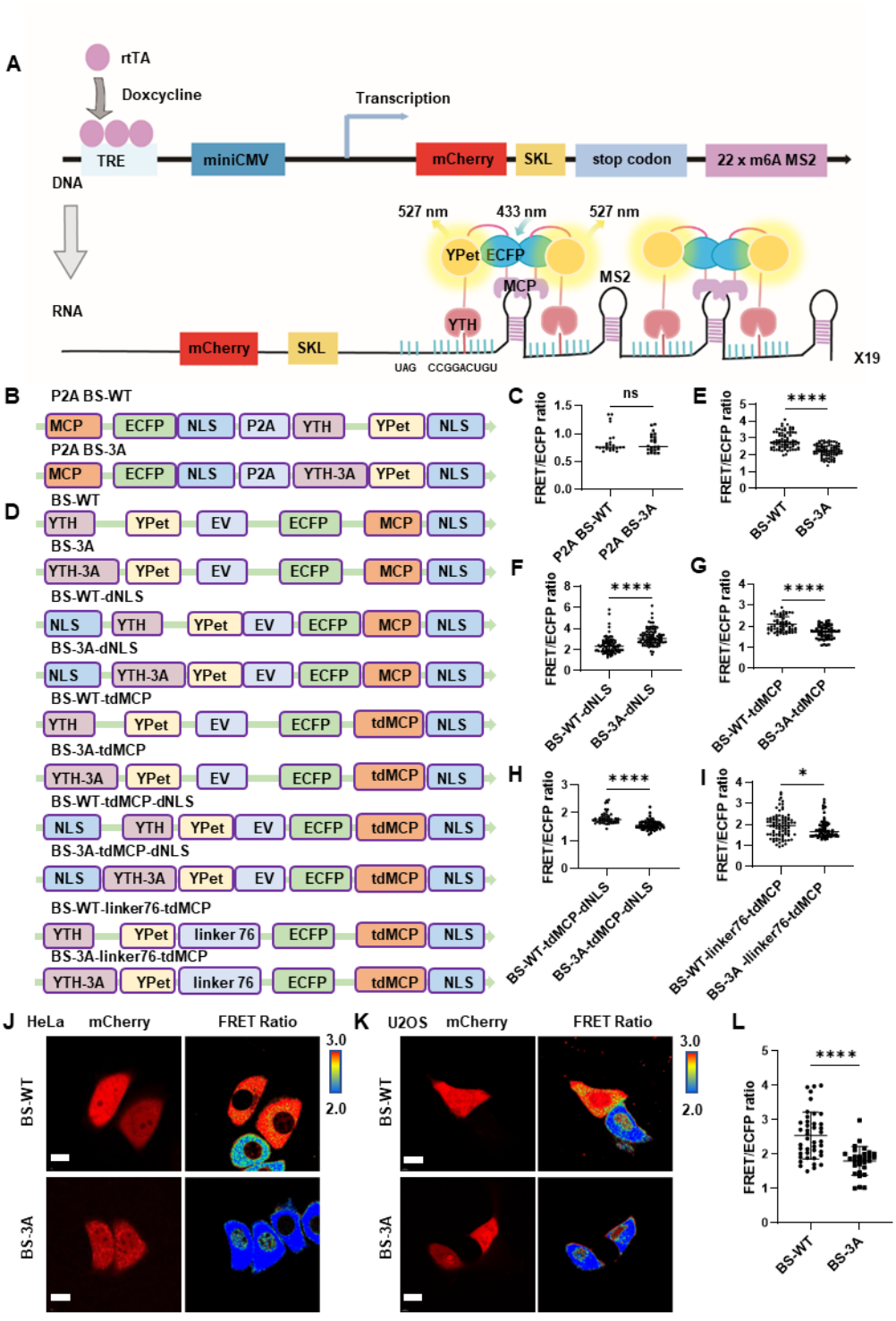

Fig. S2.

Live-cell imaging of m^{6}A modification with an mCherry reporter. (A) Schematic diagram of live-cell FRET based on genetically coding reporter RNA with the mCherry and an intramolecular FRET biosensor. **(B)** Graphical images of intermolecular FRET BS with P2A that simultaneously express MCP-ECFP-NLS and YTH-YPet-NLS or YTH-3A-Ypet-NLS. **(C)** FRET ratio after transient transfection of HeLa cells with

the mCherry reporter plasmid and P2A BS-WT or P2A BS-3A biosensor for 36 hr and DOX induction for 6 hr; unpaired *t* test with Welch's correction, P2A BS-WT: n=25; P2A BS-3A: n=22, p=0.7292. **(D)** Graphical images of various FRET biosensors. tdMCP indicates a tandem MCP, and linker 76 indicates a semiflexible linker with 76 amino acids. The FRET ratio after transient transfection of HeLa cells with the mCherry reporter plasmid and biosensors (**E**, BS-WT: n=77, BS-3A: n=81, p<0.0001), double NLS (dNLS, **F**, n=92, p<0.0001), tdMCP (**G**, BS-WT: n=61, BS-3A: n=55, p<0.0001), dNLS + tdMCP (**H**, BS-WT: n=50, BS-3A: n=63, p<0.0001), or tdMCP + linker76 (**I**, BS-WT: n=90, BS-3A: n=63, p<0.0001) for 36 hr and DOX induction for 6 hr, all the data were analyzed by unpaired *t* test with Welch's correction. **(J)** Representative images of mCherry and the FRET/ECFP ratio for (**E**); scale bar: 15 μm. **(K)** Representative images of mCherry and the FRET/ECFP ratio after transient transfection of U2OS cells with the mCherry reporter RNA plasmid and BS-WT or BS-3A biosensor for 36 hr and DOX induction for 6 hr; scale bar: 15 μm. **(L)** FRET/ECFP ratio for (**K**), unpaired *t* test with Welch's correction, BS-WT: n=42, BS-3A: n=29, p<0.0001. *ns*: not significant.

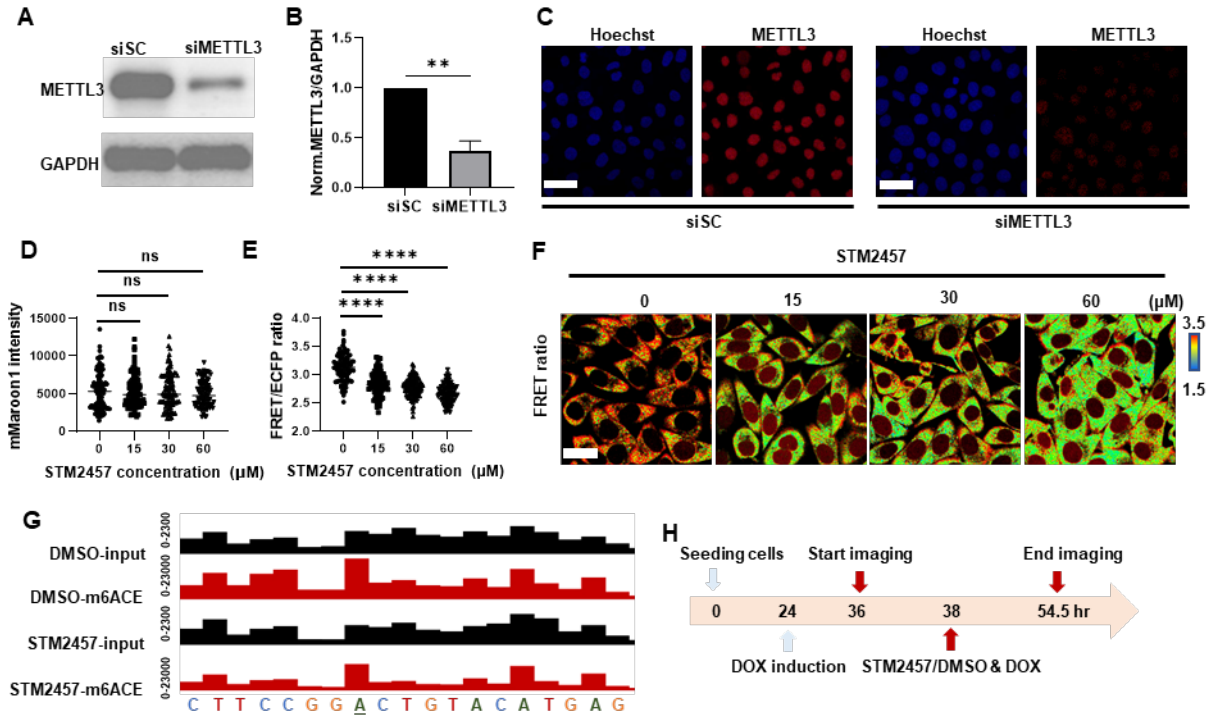

Fig. S3.

siMETTL3 and inhibitor STM2457 efficiently reduced METTL3 level and activity. (A) Western blot of GAPDH and METTL3 after siSC and siMETTL3 treatment. **(B)** Normalized METTL3/GAPDH expression in HeLa cells after siRNA treatment; unpaired *t* test with Welch's correction, n=3, p=0.008. **(C)** METTL3 immunostaining after siSC and siMETTL3 treatment; scale bar: 50 μm. (**D**) mMaroon1 intensity of SMIS-WT cells after pretreatment with indicated concentration of STM2457 for 3 hr and incubation with indicated concentration of STM2457 and DOX (1 μg/mL) for 12 hr, unpaired *t* test with Welch's correction, n=100, 15 μM group: p=0.7769; 30 μM group: p=0.7714; 60 μM group: p=0.2341. (**E**) FRET ratio of SMIS-WT cells after pretreatment with indicated concentration of STM2457 for 3 hr and incubation with indicated concentration of STM2457 and DOX (1 μg/mL) for 12 hr, unpaired *t* test with Welch's correction, n=100, p<0.0001. (**F**) Representative FRET images of SMIS-WT cells after pretreatment with indicated concentration of STM2457 for 3 hr and incubation with indicated concentration of STM2457 and DOX (1 μg/mL) for 12 hr, scale bar: 20 μm. **(G)** m6ACE (red) and Input (black) read-start counts (in reads per million mapped or RPM) mapped to mMaroon1 reporter gene, showed as zoom-in view, the peak count range of input and m6ACE is 0-2300 and 0-23000, respectively, m^{6}A site is marked with an underline. (H) FRET imaging procedure of SMIS-WT cells after STM2457 or DMSO treatment. Specifically, SMIS-WT cells was induced by DOX for 14 hours before treatment with STM2457/DMSO and DOX for another 16.5 hr. The FRET imaging started at 36 hr and ended at 54.5 hr.

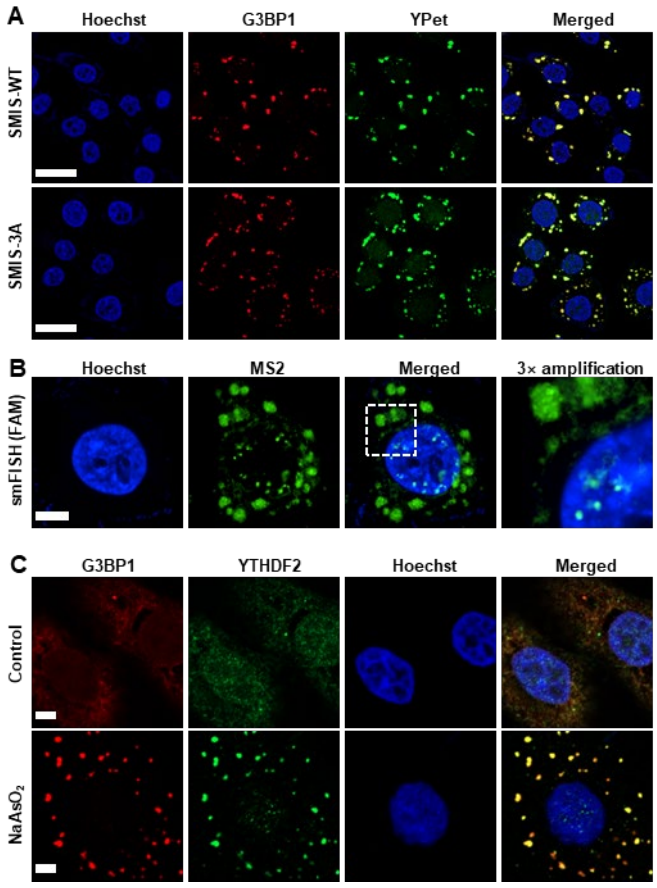

Fig. S4.

mMaroon1 reporter RNA is enriched in SGs. (A) G3BP1 immunostaining images and YPet images of SMIS-WT and SMIS-3A cells after DOX induction for 12 hr and $NaAsO_2$ treatment for 1 hr; scale bar: 50 μm. **(B)** smFISH of reporter mRNA in m^6A reporter cells after DOX induction for 12 hr and $NaAsO_2$ treatment for 1 hr; scale bar: 5 μm. The white square with dashed lines indicates the region for 3× amplification; antisense DNA oligo for smFISH: FAM-GACATGGGTGATCCTCATGT-FAM. **(C)** G3BP1 and YTHDF2 immunostaining images of HeLa cells after $NaAsO_2$ treatment for 1 hr; scale bar: 5 μm.

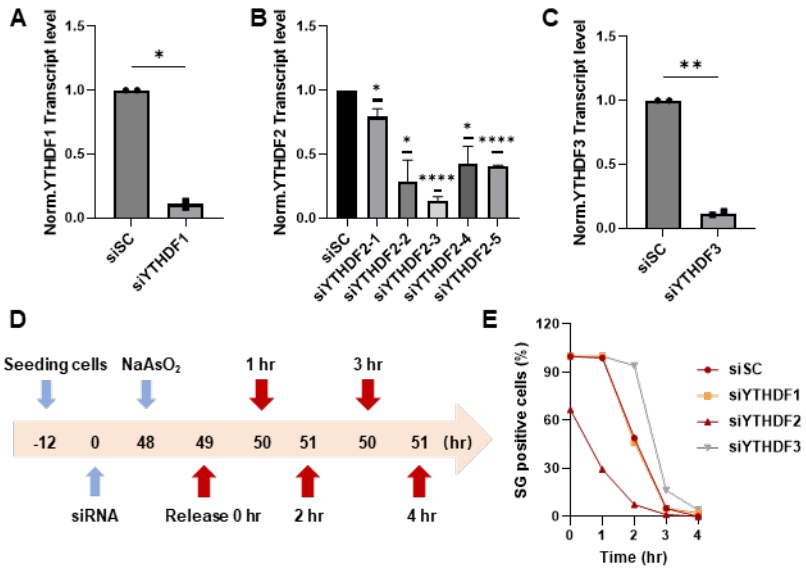

Fig. S5.

Screening siRNAs for YTHDFs to regulate SG disassembly. The normalized transcript level of YTHDF1 (**A**), YTHDF2 (**B**), and YTHDF3 (**C**) after siRNA treatment; unpaired *t* test with Welch's correction, siYTHDF1, n=2, p=0.0179; siYTHDF2-1, n=3, p=0.028; siYTHDF2-2, n=3, p=0.0176; siYTHDF2-3, n=3, p<0.0001; siYTHDF2-4, n=3, p=0.0179; siYTHDF2-5, n=3, p<0.0001 and siYTHDF3, n=2, p=0.0094. **(D)** The workflow of G3BP1 immunostaining in HeLa cells after siRNA treatment during SG formation and disassembly. **(E)** The percentage of SG-positive HeLa cells during SG recovery following the workflow of (**D**).

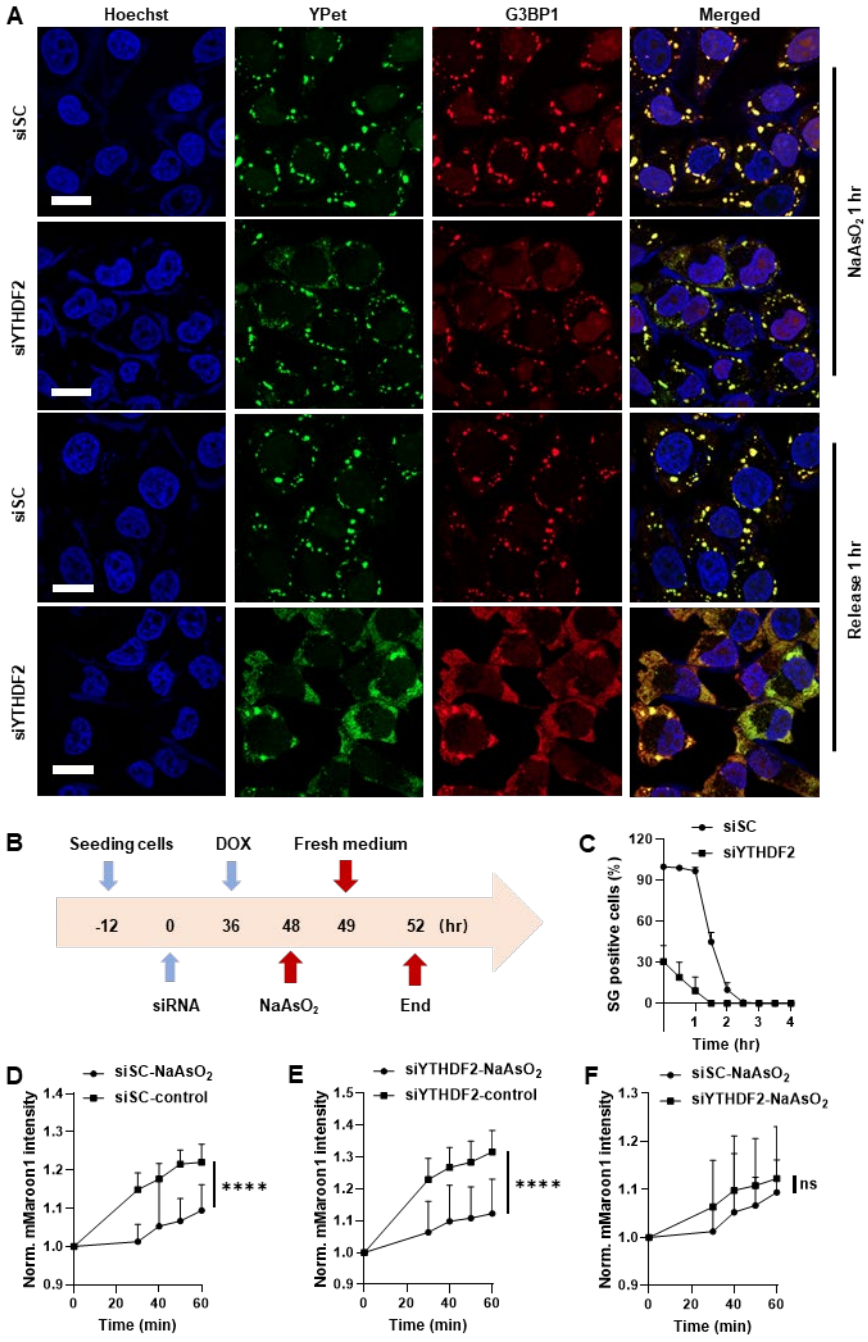

Fig. S6.

SMIS was used to monitor the SG dynamics and translation of mMaroon1 after YTHDF2 knockdown. (A) G3BP1 immunostaining and YPet images of the SMIS-WT after siSC or siYTHDF2 treatment for 36 hr, DOX induction for 12 hr, $NaAsO_2$ treatment for 1 hr and release for 1 hr; scale bar: 20 μm. **(B)** The workflow of time-lapse imaging of SG formation and disassembly. First, the SMIS-WT cells were seeded on glass bottom dishes for 12 hr, transfected with siRNAs for 36 hr, treated with fresh medium supplemented with 1 μg/mL DOX and siRNAs for another 12 hr, then change the media and incubated with fresh medium supplemented with 0.5 mM $NaAsO_2$ for 1hr, and then washed out $NaAsO_2$ and incubated with fresh medium and siRNAs for 3 hr. The imaging started from the beginning of the $NaAsO_2$ treatment

(t=48 hr) and continued to the end (t=52 hr). **(C)** Percentage of SG-positive SMIS-WT cells after siRNA treatment and release from $NaAsO_2$; n=4. **(D)** mMaroon1 intensity normalized to that at 0 min after $NaAsO_2$ addition or without treatment in SMIS-WT cells after siSC treatment; unpaired *t* test with Welch's correction, n=30, $p<0.0001$. **(E)** mMaroon1 intensity normalized to that at 0 min after $NaAsO_2$ addition or without treatment in SMIS-WT cells after siYTHDF2 treatment; unpaired *t* test with Welch's correction, n=30, $p<0.0001$. **(F)** mMaroon1 intensity was normalized to that at 0 min after $NaAsO_2$ addition to SMIS-WT cells after siSC or siYTHDF2 treatment for 36 hr, DOX induction for 12 hr and $NaAsO_2$ treatment (unpaired *t* test with Welch's correction, n=30, $p=0.225$). *ns*: not significant.

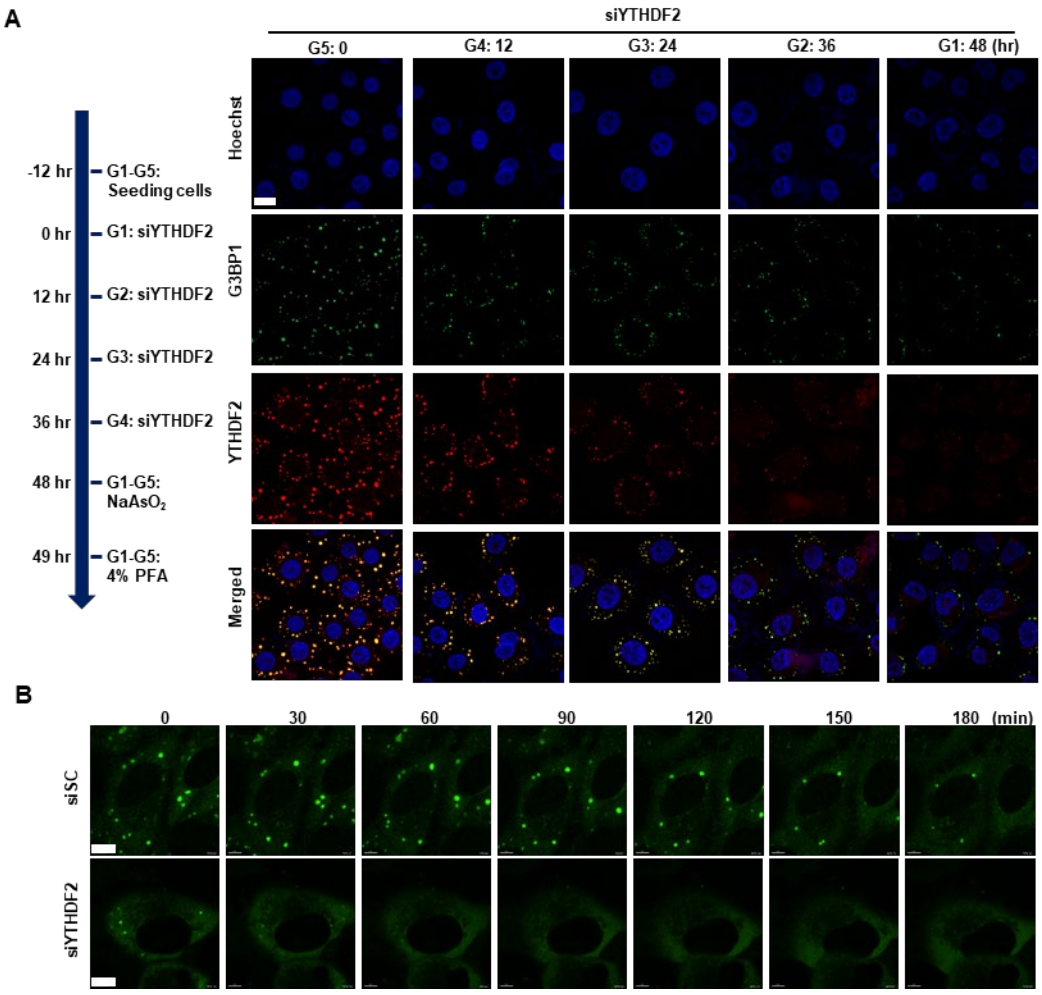

Fig. S7.

Highly efficient YTHDF2 knockdown reduces SG stability. (A) YTHDF2 and G3BP1 immunostaining in HeLa cells after siYTHDF2 treatment at the indicated time points; scale bar: 20 μm; G1-G5: G1-5 in which cells are treated with siYTHDF2 for 48, 36, 24, 12, and 0 hr, respectively. **(B)** Live-cell imaging of G3BP1-EGFP in U2OS cells during $NaAsO_2$ release after siSC or siYTHDF2 treatment; scale bar: 20 μm.